

Conventional and advanced exergy analysis of a vehicular proton exchange membrane fuel cell power system

Zhiqiang Liu^a, Longquan Li^a, Chengwei Deng^b, Jingzheng Ren^c, Yi Sun^b, Zhenyu Xiao^a, Sheng Yang^{a,*}

^aSchool of Energy Science and Engineering, Central South University, Changsha 410083, People's Republic of China

^bSpace Power Technology State Key Laboratory, Shanghai Institute of Space Power-Sources, Shanghai 200245, People's Republic of China

^cDepartment of Industrial and System Engineering, Hong Kong Polytechnic University, Hong Kong SAR, China

***Corresponding author:**

Sheng Yang

ceshyang@csu.edu.cn

Abstract

Proton exchange membrane fuel cell powered vehicles have received lots of attention due to various merits and are currently in the initial stage of commercialization. A comprehensive proton exchange membrane fuel cell power system with heat recovery for reactants preheating is proposed and investigated. Different with previous literatures, the heat exchangers for reactant preheating are parallel-arranged. Thermodynamic model is established to simulate the system process and the model is validated rigorously. By a parameter study, an acceptable interval of stream separation ratio for the parallel-arranged heat exchangers in this system varies from *0.24* to *0.56*. Conventional and advanced exergy analyses of the system are studied. The real improvement potentials of all the components in the system are quantified: *46.42%* of the total exergy destruction is avoidable, and the improvement priority orders are given: PEMFC stack >WP>AC>R>CHE>AHE>HC. It is found that a strong intersection exists in the system since *84%* of the total exergy destruction is exogenous. Intersections of each component with the remaining components are analyzed. *87.97%* of the exergy destruction in the stack is found to be exogenous, which indicates that improvement of auxiliary components will be effective. It is also suggested that improvement of the humidifiers should be given special priority. This paper could provide directions for further improvement on efficiency of this system and deeper understandings of intersections between the components.

Key words: proton exchange membrane fuel cell system; exergy analysis; advanced exergy analysis; parallel-arranged waste heat recovery.

Nomenclature

A	effective electrode area (cm^2)
C	gas concentration (mol/cm^3)
C_p	the specific heat at constant pressure ($\text{J}/(\text{kg}\cdot\text{K})$)
d	moisture
e	specific exergy (J/kg)
E	exergy (W)
E_{ernst}	reversible voltage (V)
F	the Faraday constant
g	mass fraction
i	current (A)
l	membrane thickness (cm)
m	mass flow rate (kg/s)
M	relatively mole mass
n	number of fuel cell
P	pressure(atm)
Q	heat (W)
R	radiator
R	resistance (Ω)
R_g	the gas constant ($\text{J}/(\text{kg}\cdot\text{K})$)
RH	relative humidity
S	stoichiometric ratio
SR	Separation ratio
T	temperature (K)
V	voltage (V)
W	power (W)
<i>Greek letters</i>	
ρ_m	membrane specific resistivity ($\Omega\cdot\text{cm}$)
ρ	density
γ	adiabatic coefficient

η	efficiency (%)
ε_d	exergy destruction ratio (%)
ε_k	exergy efficiency (%)
<i>Subscripts</i>	
0	the reference state
a	anode
ac	air compressor
acp	acceptable
act	activation
ahe	anode heat exchanger
$conc$	concentration
c	cathode
ch	chemical
d	destruction
dg	dry gas
en	energy
ex	exergy
F	fuel
hc	hydrogen compressor
in	inlet
k	component number
m	mass
max	maximum
min	minimum
$others$	other components
p	parasitic
ph	physical
P	product
r	radiator
s	stack

sat saturated vapor

v water vapor

wg wet gas

wp the water pump

Superscripts

AV avoidable

ch chemical

EN endogenous

EX exogenous

sat saturation

UN unavoidable

Abbreviations

AC air compressor

AH anode humidifier

AHE anode heat exchanger

CH cathode humidifier

CHE cathode heat exchanger

HC hydrogen compressor

PEMFC proton exchange membrane fuel cell

WP water pump

1. Introduction

Polymer electrolyte membrane fuel cell (PEMFC) technologies with benefits of zero emission, high energy conversion efficiency, high power density, silent operation, high reliability and low maintenance have received world-wide attention in recent years [1-2]. Fuel cell electric vehicle is a primary area for PEMFC application, and main stakeholders, i.e. governments and vehicle manufacturer, are positively promoting the development of fuel cell vehicles [3]. PEMFC power system is a core sub-system that would directly affect performance of the overall fuel cell electric vehicles [4]. Fuel cell vehicles with a performance that are not inferior to existing vehicle on the current market are desperately desired, and efficiency improvement of the PEMFC power system could greatly accelerate the progress toward this target [5]. From a thermodynamic point of view, a complete PEMFC power plant for vehicular application consists of PEMFC stack, hydrogen processing sub-system, air processing sub-system and thermal management sub-system [6]. PEMFC stack is the core component in the plant and operation conditions could significantly affect its performance [7]. Proper operation conditions for the stack are provided by the sub-systems. Generally, air from the environment needed to be compressed, preheated and humidified in the air processing sub-system before entering the stack, while hydrogen from the high-pressure tank needed to be preheated and humidified without being compressed in the hydrogen processing system. Coolant in the thermal management brings away waste heat generated in the stack to avoid the temperature runaway [8].

Waste heat recovery of the PEMFC stack for reactants preheating is a positive strategy to improve system energy utilizing efficiency [9]. Kamil [10] experimentally investigated the opportunities for improving the performance of an open cathode PEMFC by capturing heat generated in the fuel cell for preheating the inlet hydrogen. The results showed that depending on the stack power output, by using 3–6% of the heat generated by the fuel cell, the hydrogen temperature could be increased in the range of 2–13 °C, and consequently the stack power could be increased by up to 10%.

The high-temperature coolant from the stack outlet could be also utilized to preheat both reactants, and two heat exchangers are needed for air and hydrogen preheating respectively. Apparently, heat exchangers in cathode and anode could be arranged either in series or in parallel. The series-arranged heat exchangers for heat recovery has been studied in [11], however, the parallel-arranged ones have not been investigated yet to the best of our knowledge.

Exergy analysis is a useful theoretical tool to guide system energy conversion efficiency improvement from the thermodynamic point of view [12]. Conventional exergy method has been widely applied to analyze PEMFC power system. M.M. Hussain et.al [13] conducted thermodynamic analysis on a PEMFC power system, they found that system energy and exergy efficiency would climb up to their peak values and then decrease as the stack current density being gradually increased, which could be understood as: when the current density is increased, parasitic power in the auxiliary components and power generated in the stack are increased simultaneously, and the former is even greater when the current is large enough. S.O.Mert [14-15] examined the performance of a Ballard-series PEMFC power system, and found that the energy and exergy efficiency of the system always decrease as the current density is increased, this trend difference with that in [13] could result from the different system layout and parameters. In another study on high-temperature PEMFC system by Lin Ye et.al [16], the same tendency with that by S.O.Mert was discovered. More recently, Guokun Liu et.al [11] presented thermodynamic and exergy analysis on the PEMFC power system, and found that a maximum energy and exergy efficiency appears when stack operating temperature is increased gradually.

Compared with conventional exergy analysis, advanced exergy analysis method could provide more detailed and reliable results. The method was first proposed by Tsatsaronis et.al [17] and this research group further developed this method in analysis of different energy systems [18-24]. Taking the unavoidable exergy destruction caused by technical and economic limitations into consideration, exergy destruction is divided into avoidable and unavoidable part. Thus, the real improvement of the energy system could be quantified. By splitting exergy

destruction into exogenous and endogenous part, interactions between components could be analyzed [25]. This method has been applied to many other energy systems and more instructive results were found for further optimization of these systems [26-32]. Recently, advanced exergy analysis has been applied in fuel cell related systems. M.shaygen et.al [33] conducted advanced exergy analysis on a hybrid regenerative PEMFC system, where an electrolyser and a photovoltaic cell provide hydrogen for the PEMFC. However, necessary auxiliary components for the PEMFC are neglected in this study. M. Fallah et.al [34-35] conducted advanced exergy analysis on an anode gas recirculation solid oxide fuel cell system. In their studies, different methods for exogenous and endogenous exergy division, i.e. engineering method and modified hybrid method, are compared. The unavoidable condition of the solid oxide fuel cell was determined by adopting internal geometric parameters of the fuel cell that result in an optimum performance. However, advanced exergy analysis for the vehicular PEMFC power system containing different auxiliary components has not been investigated so far to the best of our knowledge.

Based on above elaborated research background, main contributions and innovations in this paper could be expressed as below: A comprehensive PEMFC system with different auxiliary components is systematically analyzed. The heat exchangers in anode and cathode are parallel-arranged for waste heat recovery, and this strategy is investigated for the first time. A steady-state thermodynamic model of the PEMFC power system is established and validated rigorously. Based on the model, effect of the separation ratio for anode and cathode heat exchangers is investigated. In order to reveal more detailed thermodynamic information and provide more reliable guidance on direction for further optimization of this system, conventional and advanced exergy analyses are conducted on the system. This is the first time that advanced exergy analysis of this system is presented and this could fulfill the research gap in this field. The following parts of this paper are organized as: in Section 2, layout of the proposed system and governing equations of all the components are presented to constitute the simulation model. By the simulation model, the thermodynamic properties at all the state points in the system could be calculated. In

Section 3 introduces the conventional and advanced exergy analysis method adopted in this paper in detail. Section 4 provides results and discussion of the parametric study conventional exergy analyses and advanced exergy analysis. Finally, this work is concluded in Section 5.

2. System layout and simulation modeling

2.1. System layout

To provide a proper operating condition, hydrogen from the high-pressure hydrogen tank and air from the environment should be processed before entering the PEMFC stack, and waste heat generated in the stack should be taken away. Thus, PEMFC stack, hydrogen processing sub-system, air processing sub-system and thermal management system are necessary to constitute a comprehensive PEMFC power system. The stack plays a core role in this system, which is connected to three sub-systems simultaneously.

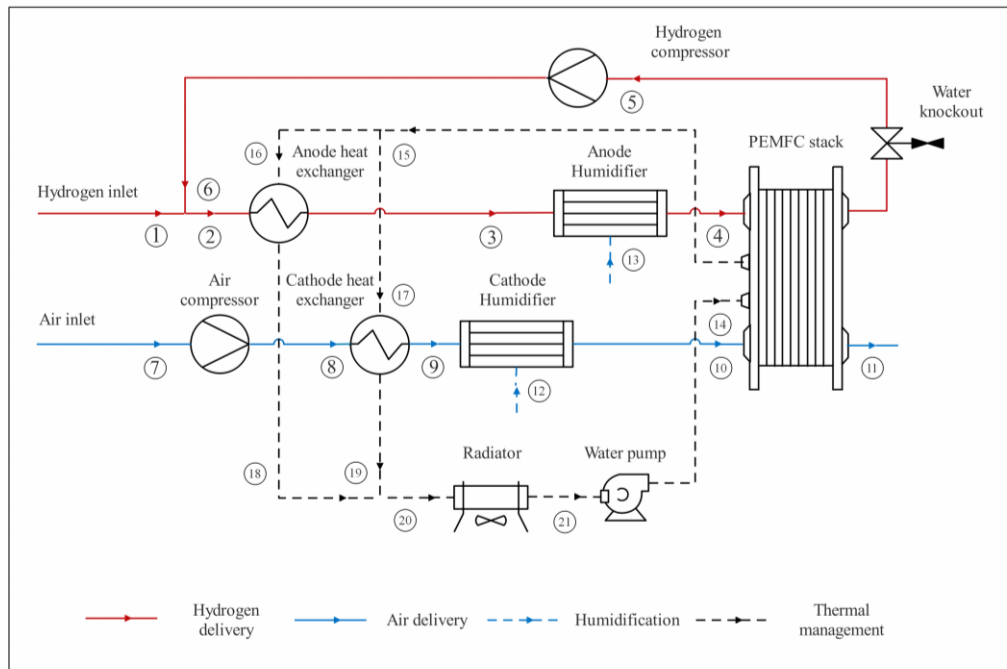


Fig.1. System layout of a PEMFC system

Air processing sub-system, indicated by blue lines in Figure 1, consists of air compressor (AC), cathode heat exchanger (CHE) and cathode humidifier (CH). Air

from the environment is compressed to reach the inlet pressure of the stack. Then the compressed air is preheated by the high-temperature coolant from the stack. Before entering the stack, reactant air has to be humidified to improve the proton conductivity of the proton exchange membrane. Although different kinds of humidification methods, e.g. bubbling method, enthalpy wheel method, direct water injection method, membrane humidification method and internal humidification methods, have been proposed [36], direct water or steam injection method is selected in the present work for its reliable performance and technology mature extent in practice. Air temperature should be higher than stack inlet temperature since a temperature drop would happen in the humidifier.

In hydrogen processing sub-system, indicated by red lines in Figure 1, hydrogen circulation anode strategy [4], is adopted for hydrogen management. Excess hydrogen from the stack anode outlet is compressed to reach the stack inlet pressure in hydrogen compressor (HC), and then mixed with hydrogen from the pressure adjustment valve of the onboard hydrogen storage tank. The mixed hydrogen flows through the anode heat exchanger (AHE) and the anode humidifier (AH) in sequence before entering the stack.

Thermal management sub-system, indicated by dotted black lines in Figure 1, consists of water pump (WP), AHE, CHE, and radiator (R). The coolant at the stack inlet temperature absorbs waste heat generated in the stack and experiences a temperature rise. The high-temperature coolant release part of the water heat through AHE and CHE to preheat the reactants, and then get cooled in R. It should be noted that AHE and CHE are arranged in parallel instead of the series-arranged one in Ref [11] Power required in the thermal management system is provided by WP.

2.2. Thermodynamic modeling

In order to simplify the thermodynamic model and make advanced exergy analysis feasible, several reasonable assumptions are made:

- (1) The system works under steady state conditions. [11]
- (2) Kinetic and potential energy of the fluids are negligible. [11]

- (3) Dry air and hydrogen behave as ideal gas. [11]
- (4) Performance uniformity of fuel cells is promised in PEMFC stack. [37]
- (5) Taking uniformity of temperature distribution of the stack into consideration, temperature rise of coolant and both reactants in the stack is fixed at 5K. [11]
- (6) Heat generated in the stack is totally dissipated to the coolant water. [11]
- (7) Pressure losses in the heat exchangers and humidifiers are neglected. [25]

2.2.1. PEMFC stack

The electrochemical reactions within PEMFC can be described as [38]:

At anode



At cathode



The overall chemical reaction of PEMFC can be expressed as:



Compared with traditional combustion process [39-40], there are no excess emissions except for water in the PEMFC. Thus, the PEMFC technique is considered to be more environmental-friendly.

Despite many mathematical modeling approaches of PEMFC stack, the empirical and semi-empirical one conceived acceptance for its closeness in predicting the behavior of stack at different operating conditions. Unlike the mechanistic models, which attempt to simulate heat, mass and electrochemical phenomenon occurring within the stack, it predicts the effect of different input parameters on the $V-I$ characteristics without deep insight on the physics and electrochemical phenomenon [41]. Therefore, the empirical and semi-empirical models are convenient to analyze the stack performance at different operating condition.

The output power of the stack could be determined by [37]:

$$W_s = i_{cell} \times V_s \quad (4)$$

$$V_s = n \times V_{cell} \quad (5)$$

$$V_{cell} = E_{nemst} - V_{act} - V_{ohmic} - V_{conc} \quad (6)$$

where W_s is the stack output power in (W), i_{cell} is cell current in (A), V_s and

V_{cell} represent for stack output voltage and single fuel cell output voltage in (V), n is number of the single fuel cells, E_{nernst} is the reversible voltage in (V), V_{act} , V_{ohmic} , V_{conc} represent for activation losses, ohmic losses and concentration loss in (V).

The Nernst reversible voltage could be calculated by [37] [41]:

$$E_{nernst} = 1.22 - 8.5 \times 10^{-3} (T - 298.15) + 4.3085 \times 10^{-5} T (\ln(P_{H_2}) + \ln(0.5P_{H_2})) \quad (7)$$

$$P_{H_2} = 0.5 RH_a P_{H_2O}^{sat} \left(\frac{RH_a P_{H_2O}^{sat}}{P_a} \exp \left(\frac{1.635 i_{cell}}{AT^{1.334}} \right) - 1 \right)^{-1} \quad (8)$$

$$P_{O_2} = RH_c P_{H_2O}^{sat} \left(\frac{RH_c P_{H_2O}^{sat}}{P_c} \exp \left(\frac{4.192 i_{cell}}{AT^{1.334}} \right) - 1 \right)^{-1} \quad (9)$$

$$\log_{10}(P_{H_2O}^{sat}) = 2.95 \times 10^{-2} (T - 273.15) - 9.19 \times 10^{-5} (T - 273.15)^2 + 1.44 \times 10^{-7} (T - 273.15)^3 - 2.18 \quad (10)$$

where P_{H_2} , P_{O_2} are partial pressures of hydrogen and oxygen in (atm), T is the stack inlet temperature in (K), RH_a , RH_c are relative humidity of vapor in anode and cathode, P_a , P_c are anode and cathode inlet pressure in (atm), A is effective electrode area in (cm²), $P_{H_2O}^{sat}$ is the saturation pressure of water vapor in (atm).

The activation losses could be calculated by [41]:

$$V_{act} = \varepsilon_1 + \varepsilon_2 T + \varepsilon_3 T \ln(C_{O_2}) + \varepsilon_4 T \ln(i_{cell}) \quad (11)$$

$$C_{O_2} = \frac{P_{O_2}}{5.08 \times 10^6 \times \exp(-498/T)} \quad (12)$$

where C_{O_2} represents the concentration of oxygen at catalytic interface of the cathode in (mol/cm³)

The ohmic loss could be calculated by [37]:

$$V_{ohmic} = i_{cell} (R_m + R_c) \quad (13)$$

$$R_m = \rho_m \frac{l}{A} \quad (14)$$

$$\rho_m = \frac{181.6(1 + 0.03(\frac{i_{cell}}{A}) + 0.062(\frac{T}{303})^2(\frac{i_{cell}}{A})^{2.5})}{(\lambda - 0.634 - \frac{3i_{cell}}{A}) \exp(4.18(T - 303)/T)} \quad (15)$$

where R_m , R_c are the electronic and ionic resistances in (Ω), ρ_m is membrane specific resistivity in ($\Omega \cdot \text{cm}$), l is the membrane thickness in (cm)

The concentration loss could be calculated by [41]:

$$V_{conc} = B \times \ln (1 - i_{cell}/i_{max}) \quad (16)$$

where i_{max} is the maximum cell current in (A)

There are still seven unknown semi-empirical coefficients, i.e. $\varepsilon_1, \varepsilon_2, \varepsilon_3, \varepsilon_4, R_c, B$ and λ . The parameter estimation techniques have been developed to determine the value of these unknown parameters [37]. Values of these semi-empirical coefficients in present model are extracted from the results of a previous parameter estimation research in [41].

Mass flow rate of the reactants at the stack inlet could be calculated by [11]:

$$m_{H_2,in} = S_a M_{H_2} \frac{n_{i_{cell}}}{2F} \quad (17)$$

$$m_{Air,in} = S_c M_{O_2} \frac{n_{i_{cell}}}{4Fg_{O_2}} \quad (18)$$

where $m_{H_2,in}$, $m_{Air,in}$ are the hydrogen and air inlet mass flow rate at (kg/s), S_a , S_c are anode and cathode stoichiometric ratios, M_{H_2} , M_{O_2} are relatively mole mass of hydrogen and oxygen, F is the Faraday constant, g_{O_2} is oxygen mass fraction of air.

In addition, mass flow rate of the coolant could be calculated by [11]:

$$Q_s = n \times i_{cell} \times (E_{nernst} - V_{cell}) \quad (19)$$

$$m_{coolant} = \frac{Q_s}{C_{p,14}(T_{15} - T_{14})} \quad (20)$$

where Q_s is heat generated in the stack in (W), $m_{coolant}$ is the mass flow rate of the coolant in (kg/s).

2.2.2. Humidifiers

The humidification process in the direct water injection humidifier follows the conservation of energy [11]:

$$m_3 C_{p,3} T_3 + m_{13} C_{p,13} T_{13} = m_4 C_{p,4} T_4 \quad (21)$$

$$m_9 C_{p,9} T_9 + m_{12} C_{p,12} T_{12} = m_{10} C_{p,10} T_{10} \quad (22)$$

Vapor mass flow rate injected to the humidifier could be calculated by [11]:

$$d = \frac{M_v}{M_{dg}} \frac{RH \times P_s}{P_{wg} - RH \times P_s} \quad (23)$$

$$m_v = m_{dg} \times d \quad (24)$$

where M_v , M_{dg} are the relative molecular mass of water vapor and dry gas, RH is the relative humidity, P_s , P_{wg} are the saturated vapor pressure and wet gas pressure in (atm), d is the moisture of the wet gas, m_v , m_{dg} are mass flow rate of water vapor and dry gas in (kg/s).

Property of the wet gas could be calculated by [11]:

$$C_{p,wg} = C_{p,dg} \frac{m_{dg}}{m_{wg}} + C_{p,v} \frac{m_v}{m_{wg}} \quad (25)$$

2.2.3. Compressors and pump

Processes in compressors and pump [42] are thought to be adiabatic and isothermal respectively. Temperature at the outlet of the compressors with a certain adiabatic coefficient could be calculated by [25]:

$$T_6 = T_5 \left[1 + \frac{1}{\eta_{hc}} \left(\left(\frac{P_6}{P_5} \right)^\gamma - 1 \right) \right] \quad (26)$$

$$T_8 = T_7 \left[1 + \frac{1}{\eta_{ac}} \left(\left(\frac{P_8}{P_7} \right)^\gamma - 1 \right) \right] \quad (27)$$

Corresponding power consumed in the compressors could be calculated by [25]:

$$W_{ac} = m_7 \frac{\gamma R_g T_7}{(\gamma-1)\eta_{ac}} \left[\left(\frac{P_8}{P_7} \right)^\gamma - 1 \right] \quad (28)$$

$$W_{hc} = m_5 \frac{\gamma R_g T_5}{(\gamma-1)\eta_{hc}} \left[\left(\frac{P_6}{P_5} \right)^\gamma - 1 \right] \quad (29)$$

Power consumed by the water pump with a certain isothermal efficiency could be calculated by [11]:

$$W_{wp} = \frac{m_{coolant}(P_{14}-P_{21})}{P_{21}\eta_{wp}} \quad (30)$$

where η_{hc} , η_{ac} , η_{wp} are efficiency of the hydrogen compressor, air compressor and water pump.

2.2.4. Heat exchanger and radiator

Heat exchangers in the hydrogen processing sub-system and the air process sub-system are parallel arranged. Mass flow rate distribution for anode and cathode reactant preheating is determined by:

$$m_{16} = SR \cdot m_{15} \quad (31)$$

$$m_{17}=(1-SR)\cdot m_{15} \quad (32)$$

where SR is the separation ratio.

Since the reactants would get cooled in the humidifiers and a minimum heat transfer temperature difference exists in CHE and AHE, the heat exchangers themselves are not able to heat the reactants to the required temperature. Thus, the embedded electric heaters in the exchangers are needed. The reactants are heated to the hypothetical temperature by the high-temperature coolants, i.e. $T_{3,h}$, $T_{9,h}$, and then get heated to the required temperature by the electric heater. Energy conservation in the exchangers could be expressed as [25] [43]:

$$m_{16}C_{p,16}(T_{16}-T_{18})=m_2C_{p,2}(T_{3,h}-T_2) \quad (33)$$

$$m_{17}C_{p,17}(T_{17}-T_{19})=m_8C_{p,8}(T_{9,h}-T_8) \quad (34)$$

Performance of the heat exchangers is indicated by the minimum heat transfer temperature difference:

$$\Delta T_{c,min}=T_{18}-T_{3,h} \quad (35)$$

$$\Delta T_{c,min}=T_{19}-T_{9,h} \quad (36)$$

Power consumed by the exchangers could be calculated by:

$$W_{che}=m_8C_{p,9,h}(T_9-T_{9,h}) \quad (37)$$

$$W_{ahe}=m_2C_{p,3,h}(T_3-T_{3,h}) \quad (38)$$

Coolant is further cooled to the stack inlet temperature in the radiator. Heat loss in the radiator could be expressed as:

$$Q_r=m_{20}C_{p,20}(T_{20}-T_{21}) \quad (39)$$

2.2.5. Separation and mixer

For the hydrogen mixing process, gas 1 is the dry hydrogen from the outlet of a pressure regulating valve, whose pressure equals to the stack inlet pressure. Pressure of gas 6 at outlet of the HC equals the stack inlet pressure as well. Thus, pressure remains unchanged in the hydrogen mixer.

$$P_1=P_2=P_6 \quad (40)$$

Mass and energy conservation equation could be expressed as [25]:

$$m_1 + m_6 = m_2 \quad (41)$$

$$m_1 C_{p,1} T_1 + m_6 C_{p,6} T_6 = m_2 C_{p,2} T_2 \quad (42)$$

For the water separation process,

$$m_{16} + m_{17} = m_{15} \quad (43)$$

$$m_{16} C_{p,16} T_{16} + m_{17} C_{p,17} T_{17} = m_{15} C_{p,15} T_{15} \quad (44)$$

$$P_{16} = P_{17} = P_{15} \quad (45)$$

For the water mixing process [25],

$$m_{18} + m_{19} = m_{20} \quad (46)$$

$$m_{18} C_{p,18} T_{18} + m_{19} C_{p,19} T_{19} = m_{20} C_{p,20} T_{20} \quad (47)$$

$$P_{18} = P_{19} = P_{20} \quad (48)$$

2.2.6. Energy analysis and input data for the system

Overall energy efficiency of this system could be calculated by [11]:

$$\eta_{en} = \frac{W_{net} V_{cell}}{W_s E_{nernst}} \quad (49)$$

$$W_{net} = W_s - W_p \quad (50)$$

$$W_p = W_{ac} + W_{hc} + W_{ahe} + W_{che} + W_{wp} \quad (51)$$

where η_{en} is overall energy efficiency of the system, W_{net} is the net power of the system in (W), W_p is the parasitic power of the auxiliary components in (W).

Input data for the thermodynamic modeling of the system are shown in Table. 1.

Table.1 Input parameters for system thermodynamic modeling

Components	Parameters	Value
PEMFC stack	Number of fuel cells	120 [11]
	Effective working area	311.88 cm ² [11]
	Anode stoichiometry	1.05 [11]
	Anode inlet pressure	1.2 atm [11]
	Anode outlet pressure	1.0 atm [11]
	Anode relative humidity	100 % [11]
	Cathode stoichiometry	2.0 [11]
	Cathode inlet pressure	1.2 atm [11]
	Cathode outlet pressure	1.0 atm [11]
	Cathode relative humidity	100 % [11]
	Inlet temperature	333.15 K [11]

	Outlet temperature	338.15 K [11]
	Maximum current	360 A [11]
	Membrane thickness	178 μm [41]
	Semi-empirical parameters ε_1	-1.0431 [41]
	Semi-empirical parameters ε_2	3.7556×10^{-3} [41]
	Semi-empirical parameters ε_3	9.8×10^{-5} [41]
	Semi-empirical parameters ε_4	1.1888×10^{-4} [41]
	Semi-empirical parameters R_c	1×10^{-4} [41]
	Semi-empirical parameters B	0.0136 [41]
	Semi-empirical parameters λ	24 [41]
Compressors	Adiabatic coefficient	0.55 [11]
	Isothermal coefficient	0.43 [11]
Water pump	Inlet pressure	1.0 atm [11]
	Outlet pressure	4.0 atm [11]
	Air inlet temperature	298.15 K [11]
	Air inlet pressure	1.0 atm [11]
System inlet	Hydrogen inlet temperature	298.15 K [11]
	Hydrogen inlet pressure	1.2 atm [11]
	Water vapor temperature	298.15 K [11]
	Water vapor pressure	0.0313 atm [11]
Heat exchangers	Minimum heat exchange temperature difference	10 K [26]

3. Exergy analysis

Exergy is defined as the portion of energy that can be converted into useful work during a process with completely reversible change with the environment [12]. A standard environment should be defined first and all subsequent calculations are based on this standard environment. The present work takes the state of $T_0=298.15\text{K}$, $P_0=1\text{ atm}$ as the standard environment. To conducted exergy analysis on a thermal system, mass flow exergy and energy flow exergy should be considered.

Mass flow exergy can be divided into four parts: physical exergy, chemical exergy, kinetic exergy and potential exergy. Since kinetic energy and potential energy of fluids are neglected, the specific exergy could be calculated as the sum of specific physical exergy and specific chemical exergy in the PEMFC power system by [25]:

$$E_m = me \quad (52)$$

$$e = e_{ph} + e_{ch} \quad (53)$$

$$e_{ph} = \sum [(h_i - h_0) - T_0(s_i - s_0)] \quad (54)$$

$$e_{ch} = (\sum x_i e_i^{ch} + RT_0 \sum x_i \ln x_i) \quad (55)$$

Specific chemical exergy e_i^{ch} of the substances in the present work could be found in [11]. Since there is no chemical reaction takes place in the thermal management sub-system, the chemical exergy of the coolant water do not need to be considered in the exergy analysis.

Energy flow exergy consists of exergy of work and exergy of heat. Exergy of work equals value of work itself, while exergy of heat could be calculated by [11]:

$$E_q = (1 - \frac{T_0}{T_s}) Q \quad (56)$$

where T_s is the heat source temperature in (K), Q is heat in (W)

3.1. Conventional exergy analysis

The exergy balance equation based on the ‘Fuel-Product’ concept for the k-th component could be expressed as [28]:

$$E_{F,k} = E_{P,k} + E_{d,k} + E_{loss} \quad (57)$$

The exergy efficiency is:

$$\varepsilon_k = \frac{E_{P,k}}{E_{F,k}} \quad (58)$$

The exergy destruction ratio is:

$$\varepsilon_d = \frac{E_{d,k}}{E_{F,k}} \quad (59)$$

Expressions for fuel exergy, product exergy and exergy loss of all components in the PEMFC system are concluded in Table 2.

Table.2 Fuel exergy, product exergy and exergy loss of different components

Components	Fuel exergy	Product exergy	Exergy losses
PEMFC stack	$E_4 + E_{10} + E_{14}$ $E_5 - E_{15} - E_{11}$	W_{stack}	0
AH	E_{13}	$E_4 - E_3$	0
CH	E_{12}	$E_{10} - E_9$	0
AHE	$E_{16} - E_{18} + W_{ahe}$	$E_3 - E_2$	0
CHE	$E_{17} - E_{19} + W_{che}$	$E_9 - E_8$	0
AC	W_{ac}	$E_8 - E_7$	0
WP	W_{wp}	$E_{14} - E_{21}$	0

HC	W_{hc}	E_6-E_5	0
R	$E_{20}-E_Q$	E_{21}	0

Exergy efficiency of the PEMFC power system is defined as [11]:

$$\eta_{ex} = \frac{W_{net}}{E_I} \quad (60)$$

3.2. Advanced exergy analysis

In advanced exergy analysis, exergy destruction obtained from the conventional exergy analysis is split into detailed parts. Results of the splitting could reveal meaningful information on interactions between components and the real improvement potential of the system. In the first level splitting, exergy destruction is split as [20]:

$$E_{d,k} = E_{d,k}^{EN} + E_{d,k}^{EX} \quad (61)$$

$$E_{d,k} = E_{d,k}^{UN} + E_{d,k}^{AV} \quad (62)$$

where $E_{d,k}^{EN}$ represents the endogenous exergy destruction which is caused by the irreversibility of the k -th component itself, while $E_{d,k}^{EX}$ represents the exogenous exergy destruction caused by irreversibility of other components in the system. By splitting of the endogenous and exogenous parts, the level of interaction between the k -th component and those remaining components could be revealed. $E_{d,k}^{AV}$ represents the part of exergy destruction that could be avoided by optimization, $E_{d,k}^{UN}$ represents the part of exergy destruction that cannot be avoided even the best technologies is utilized. By splitting of avoidable and unavoidable parts, the real improvement potential of certain component is presented.

3.2.1. Splitting of endogenous and exogenous parts

There are different approaches for splitting of the endogenous and exogenous parts, such as thermodynamic cycle method, engineering (graphical) method, exergy balance method, equivalent component method, and structural theory method [20]. Among these methods, thermodynamic cycle method and engineering method are two

main methods with acceptable accuracy. Since thermodynamic cycle method is not available for systems within which chemical reactions happens, the engineering method is adopted in the present work. The main principle of this method is calculating the endogenous exergy destruction of the k -th component by drawing a diagram as shown in Fig. 2.

Exergy balance equation of the system could be expressed as [25]:

$$E_{d,total} = E_{d,k}^{EN} + E_{d,k}^{EX} + E_{d,others} \quad (63)$$

$$E_{d,total} = E_{d,k}^{EN} + mE_{d,others} \quad (64)$$

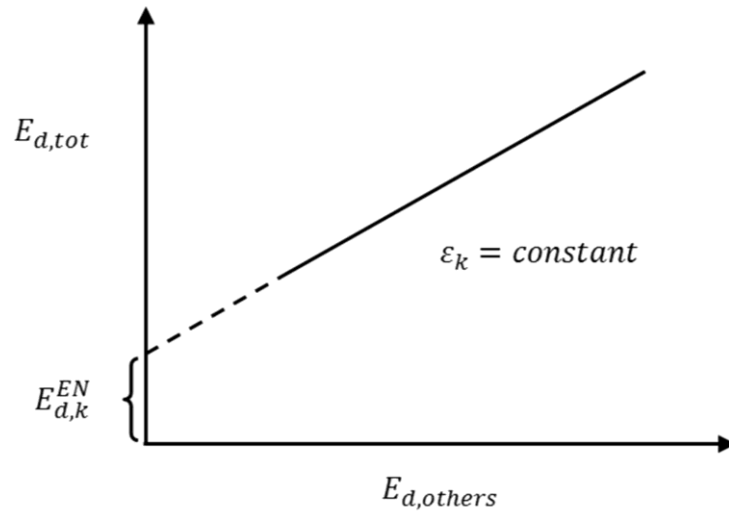


Fig.2. Illustration diagram of engineering method

From Eq. (63), it can be seen that if $\lim E_{d,others} \rightarrow 0$, then $\lim E_{d,k}^{EX} \rightarrow 0$ and $\lim E_{d,total} \rightarrow E_{d,k}^{EN}$. Also, as shown in Eq. (64) that relation between $E_{d,total}$ and $E_{d,others}$ is linear with a slope m . Demonstration of the linear trend could be found in [20]. By varying value of $E_{d,others}$, a line as shown in Fig. 2 could be plotted. The line intersects the vertical axis at a point, and the value of the resultant intercept defines the value of $E_{d,k}^{EN}$. It should be note that the exergy efficiency of the researched component should be fixed and overall system exergy production should not be changed while varying value of $E_{d,others}$.

3.2.2. Splitting of avoidable and unavoidable parts

By defining an unavoidable condition of the system where all the components operate at their highest possible efficiency. The unavoidable part of exergy destruction of the k -th component could be calculated as [26]:

$$E_{d,k}^{UN} = E_{p,k} \left(\frac{E_d}{E_p} \right)_k^{UN} \quad (65)$$

where $E_{p,k}$ is product exergy of the k -th component when the system operates under real condition in the conventional exergy analysis, $\left(\frac{E_d}{E_p} \right)_k^{UN}$ is the ratio of exergy destruction to product exergy of the k -th component when the system operates at the defined unavoidable conditions.

The most important step for splitting of avoidable and unavoidable parts is definition of the unavoidable conditions for the system. Usually, main parameters that affect the performance of the components, such as isentropic efficiency for the compressor, could be specified to define the unavoidable conditions. For PEMFC stack, lots of researches have shown that the geometric parameters, physical parameters and electrochemical parameters of internal structure in the PEMFC stack have an obvious effect on its performance [44-46]. In a multi-variable optimization work of a PEMFC stack by simulation modeling [47], nine internal structure parameters were optimized in order to obtain an optimum stack performance. According to their results, an increase of stack power output ratio of 38.87% compared with the basic case was found. In the present work, the basic case in Ref [47] is taken as the real condition, while the case where the possible optimum internal structure parameters are assumed is taken as the unavoidable conditions for the PEMFC stack. For the auxiliary components, isentropic efficiency of compressor is 90%, isothermal efficiency of water pump is 85%, minimum heat exchange temperature difference of the heat exchanger is 5K under the unavoidable conditions [26].

3.2.3. The second level splitting

In the second level, the avoidable/unavoidable concept and the

endogenous/exogenous concept is combined, the parts in Eq. (60) could be further split into more detailed parts [20]:

$$E_{d,k}^{EN} = E_{d,k}^{EN,AV} + E_{d,k}^{EN,UN} \quad (66)$$

$$E_{d,k}^{EX} = E_{d,k}^{EX,AV} + E_{d,k}^{EX,UN} \quad (67)$$

$$E_{d,k}^{AV} = E_{d,k}^{AV,EN} + E_{d,k}^{AV,EX} \quad (68)$$

$$E_{d,k}^{UN} = E_{d,k}^{UN,EN} + E_{d,k}^{UN,EX} \quad (69)$$

Recasting Eq. (60) (62) and (63), we have [21]:

$$E_{d,k} = E_{d,k}^{EN,AV} + E_{d,k}^{EN,UN} + E_{d,k}^{EX,AV} + E_{d,k}^{EX,UN} \quad (70)$$

where $E_{d,k}^{EN,AV}$ represents the endogenous avoidable part of exergy destruction that could be avoid by optimization of the k -th component itself, $E_{d,k}^{EN,UN}$ represents the endogenous unavoidable part, $E_{d,k}^{EX,AV}$ represents the exogenous avoidable part of exergy destruction that could be avoided by optimization of the remaining components in the system, $E_{d,k}^{EX,UN}$ represents the exogenous unavoidable part.

The endogenous unavoidable part of exergy destruction could be calculated by:

$$E_{d,k}^{UN,EN} = E_{d,k}^{EN} \left(\frac{E_d}{E_p} \right)_k^{UN} \quad (71)$$

4. Results and discussions

4.1. Model validation

Validation of the thermodynamic model is conducted from both the stack level and the system levels.

For validation of the PEMFC stack model, voltage-current and power-current curves from the present model are compared with that from the experimental results in [48]. Operation conditions and cell number of the present model are consistent with the experimental conditions, i.e. $T=346$ K, $P_c=250$ kPa, $P_a=285$ kPa, $n=80$. As shown in Fig. 3, a good agreement can be seen between the simulation and experimental results, the maximum error is found to be within 5%.

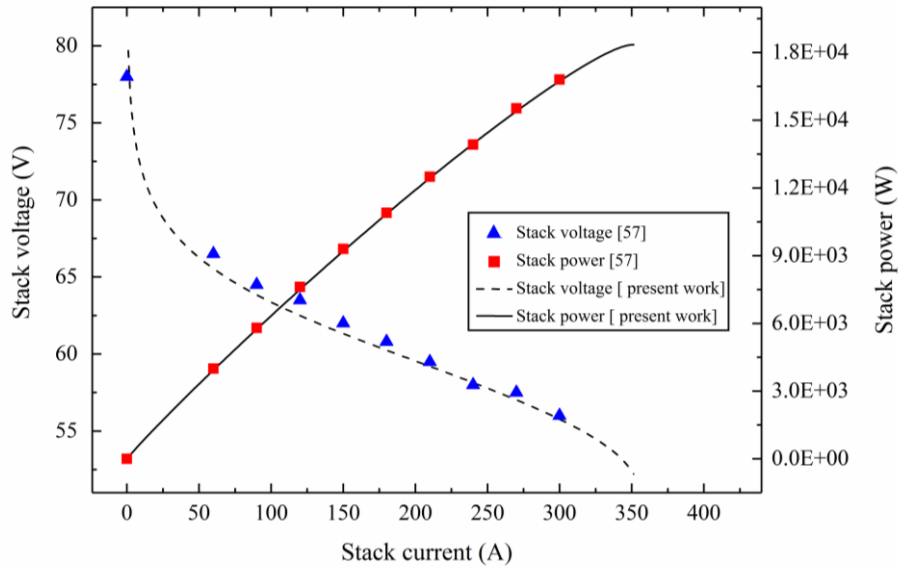


Fig.3. Validation of the PEMFC stack modeling

For validation of the overall system model validation, results of this model are compared with that of the model developed in Ref [11]. Different PEMFC stack modeling method, i. e. the flow network method, was adopted in Ref [11], and the modeling methods of some auxiliary components are different as well. Main operation parameters and system parameters are kept constant in this work and Ref [11], comparison of the two models provides evidence for validation for the present model. Since the series-arranged heat exchangers strategy was adopted in the system layout in Ref [11], thermodynamic properties at all the state points of the two systems become impossible. But the power consumptions of different components in the two systems are compared. Again, a good agreement is shown in Table 3, the maximum error is found to be within 10%.

Table.3 Comparison of power of different components at different current densities in the present work and [11]

Components	0.6 A/m ²		0.7 A/m ²		0.8 A/m ²		0.9 A/m ²		1.0 A/m ²	
	Model [11]	Present work								

PEMFC	16235	16296	18417.74	18682	20299.65	20931	22062.39	23013	23727.83	24884
stack	Error: 0.37%		Error: 1.41%		Error: 3.11%		Error: 4.13%		Error: 4.64%	
Compressors	460.87	478.22	537.68	557.534	614.5	636.85	691.3	716.06	768.12	795.38
	Error: 3.63%		Error: 3.56%		Error: 3.51%		Error: 3.46%		Error: 3.43%	
Heat exchangers	151.83	167.11	177.13	194.34	202.44	222.17	227.74	249.59	253.05	276.91
	Error: 9.14%		Error: 8.86%		Error: 8.88%		Error: 8.75%		Error: 8.62%	
Water pump	382.47	366.7	463.85	438.4	555.31	514.7	650.80	596.9	749.56	686.4
	Error: -4.3%		Error: -5.81%		Error: -7.89%		Error: -9.03%		Error: -9.21%	

4.2. Parameter study of the parallel-arranged heat recovery strategy

In the parallel-arranged heat recovery strategy, high-temperature coolant from the stack outlet (15) is separated into two flow streams (16 and 17) to preheat the hydrogen and air. Then the flow streams at the outlets of the heat exchangers (18 and 19) are mixed. Generally, a temperature difference between stream 18 and 19 would result in exergy destruction in the mixing process, and temperature consistency between stream 18 and 19 is desired. Effect of the separation ratio of the high-temperature coolant on outlet temperature of the heat exchangers is shown in Fig.4. It could be seen that an interval (0.24-0.56) of the separation ratio exists to ensure the consistency between T_{18} and T_{19} . Too large or too small separation ratio would result in the temperature difference. This would provide guidance in practical design and fabrication of such a system. In the following conventional and advanced exergy analysis, value of this separation ratio is fixed at 0.5.

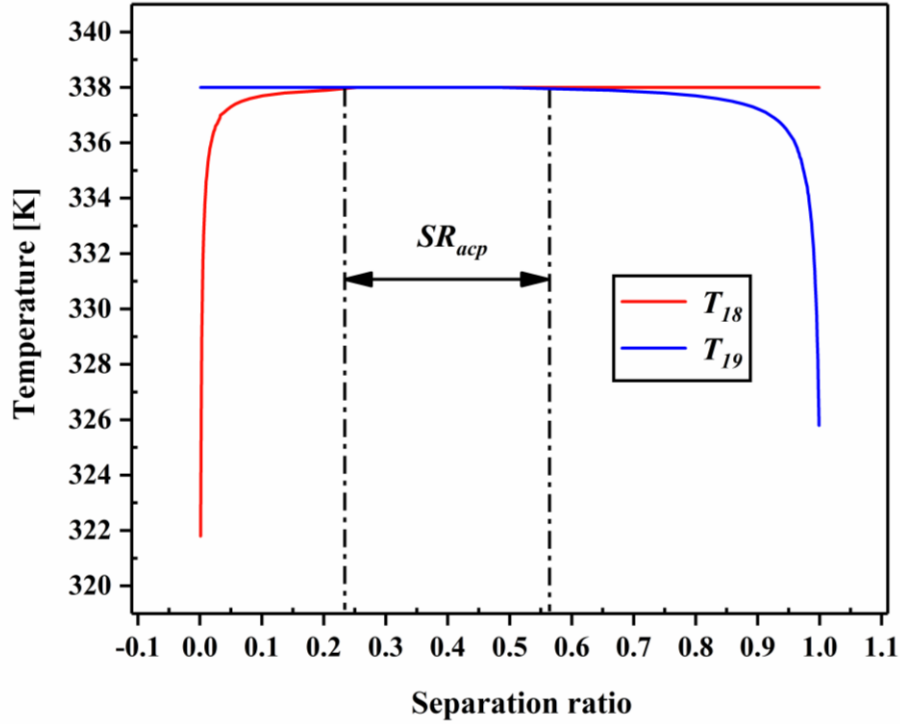


Fig.4. Effect of the separation ratio on the outlet temperature of heat exchangers

4.3. Conventional exergy analysis

Thermodynamic properties and mass flow rates at different state points of the PEMFC power system under real conditions are shown in Table 4. Some parameter in this table is consistent with that in Ref [11], which provides more evidence to the model validation to some extent. Power and conventional exergy information of different components under real conditions are shown in Table 5. As a core component in the system, PEMFC stack share the largest parts in power, fuel exergy, product exergy and exergy destruction among all the components.

Order of the remaining component in contribution to the parasitic power is: AC>WP>CHE>AHE>HC. To save the parasitic power consumption in the auxiliary components, it would be suggested that the improvement priority should be given to the components with more power consumption, e.g. AC and WP. Order of the auxiliary components in contribution to the total exergy destruction is: CH>CHE>WP>AC>AH>R>AHE>HC. To increase the system exergy efficiency, improvement priority should be given to those components with more exergy

destruction. Since energy analysis only focuses on quantity of energy, while exergy focus on both quality and quantity of energy, a different priority order is found here.

Table.4 Thermodynamic properties at different state points in the system

State point	Working fluid	Pressure (atm)	Temperature (K)	Mass flow rate (g/s)	Moisture content(-)	Exergy (W)
1	Hydrogen(dry)	1.2	298.2	0.3089	0	36535
2	Hydrogen(dry)	1.2	301	0.3243	0	38358
3	Hydrogen(dry)	1.2	341.2	0.3243	0	38371
4	Hydrogen(wet)	1.2	333.2	0.8916	1.749	38472
5	Hydrogen(dry)	1.0	338.2	0.01544	0	1824
6	Hydrogen(dry)	1.2	356.2	0.01544	0	1828
7	Air(dry)	1.0	298.2	21.49	0	0
8	Air(dry)	1.2	314.1	21.49	0	417.1
9	Air(dry)	1.2	341.3	21.49	0	424.2
10	Air(wet)	1.2	333.2	24.17	0.125	943.2
11	Air(wet)	1.0	338.2	12.09	0.125	479.1
12	Water vapor	0.0313	298.2	2.685	-	1417
13	Water vapor	0.0313	298.2	0.5673	-	299.4
14	Water	4	333.2	728	-	6024
15	Water	1.0	338.2	728	-	7505
16	Water	1.0	338.2	364	-	3753
17	Water	1.0	338.2	364	-	3753
18	Water	1.0	338.1	364	-	3738
19	Water	1.0	337.9	364	-	3716
20	Water	1.0	338	728	-	7453
21	Water	1.0	333.2	728	-	5804

Table.5 Power and conventional exergy information of different components in the system under real conditions

Components	Power (W)	E_F (W)	E_P (W)	E_d (W)	ϵ_k	ϵ_d
PEMFC stack	19879	35632	19879	15753	0.56	0.44
AH	0	299.4	100.5	198.9	0.34	0.66
CH	0	1417	519.1	898.1	0.37	0.63
AHE	61.17	76.04	13.43	62.61	0.18	0.82
CHE	289.7	326.6	7.067	319.5	0.02	0.98
AC	627	627	417.1	209.9	0.66	0.34
HC	7.315	7.315	4.028	3.287	0.55	0.45

R	0	1649	1554	95.2	0.94	0.06
WP	526.2	526.2	220.2	306	0.42	0.58

It should be noted that the cathode humidifier share the largest exergy destruction among the auxiliary components. The reason could be the low inlet temperature of the injected water vapor. Recently, the membrane humidification method has accepted lots of attention due to its possible ability for cathode exhausted gas recovery [49-53]. From the perspective of the conventional exergy analysis, development of the membrane humidification method would increase the system exergy efficiency.

4.4. Splitting of avoidable and unavoidable parts

Table.6. Power and conventional exergy information of different components in the system under unavoidable conditions

Components	Power (W)	E_F (W)	E_P (W)	E_d (W)	ε_k	ε_d
PEMFC stack	27602	35632	27602	8030	0.77	0.23
AH	0	299.4	100.5	198.9	0.34	0.66
CH	0	1417	508.7	908.3	0.36	0.64
AHE	37.89	55.51	13.47	42.04	0.24	0.76
CHE	183.2	233.1	17.6	215.5	0.08	0.92
AC	383.2	383.2	359	24.2	0.94	0.06
HC	4.47	4.47	4.028	0.442	0.90	0.10
R	0	1633	1540	93	0.94	0.06
WP	282.9	282.9	220.2	62.7	0.78	0.22

Part of the exergy destruction appears in the conventional exergy analysis is not avoidable due to technical and economical limitations. Exergy destruction of each component is split into avoidable and unavoidable part in advanced exergy analysis. Power and conventional exergy information of the different components when the system is operates at the unavoidable conditions are shown in Table 6. Combined with the results under real conditions, splitting of the avoidable and unavoidable part could be achieved, and the results are shown in Table 7.

Table.7 Results from advanced exergy analysis (W).

Components	$E_{d,k}$	$E_{d,k}^{UN}$	$E_{d,k}^{AV}$	$E_{d,k}^{EN}$	$E_{d,k}^{EX}$	$E_{d,k}^{UN,EN}$	$E_{d,k}^{UN,EX}$	$E_{d,k}^{AV,EN}$	$E_{d,k}^{AV,EX}$
PEMFC Stack	15753	8030	7723	1895.3	13857.7	427.12	7602.88	1468.18	6254.82
AH	198.9	198.9	0	68.67	130.23	45.62	153.28	23.05	-23.05
CH	898.1	898.1	0	469.1	429	297.32	800.78	171.78	-171.78
AHE	62.61	47.42	15.19	43.48	19.13	32.93	24.66	10.55	4.64
CHE	319.5	301.94	17.56	22.51	296.99	20.81	281.13	1.7	15.86
AC	209.9	13.15	196.75	209.9	0	13.15	0	196.75	0
HC	3.287	0.33	2.957	3.287	0	0.33	0	2.957	0
R	95.2	5.45	89.75	14.82	80.38	0.85	4.6	13.97	75.78
WP	306	67.73	238.27	4.26	301.74	0.94	66.79	3.32	234.95

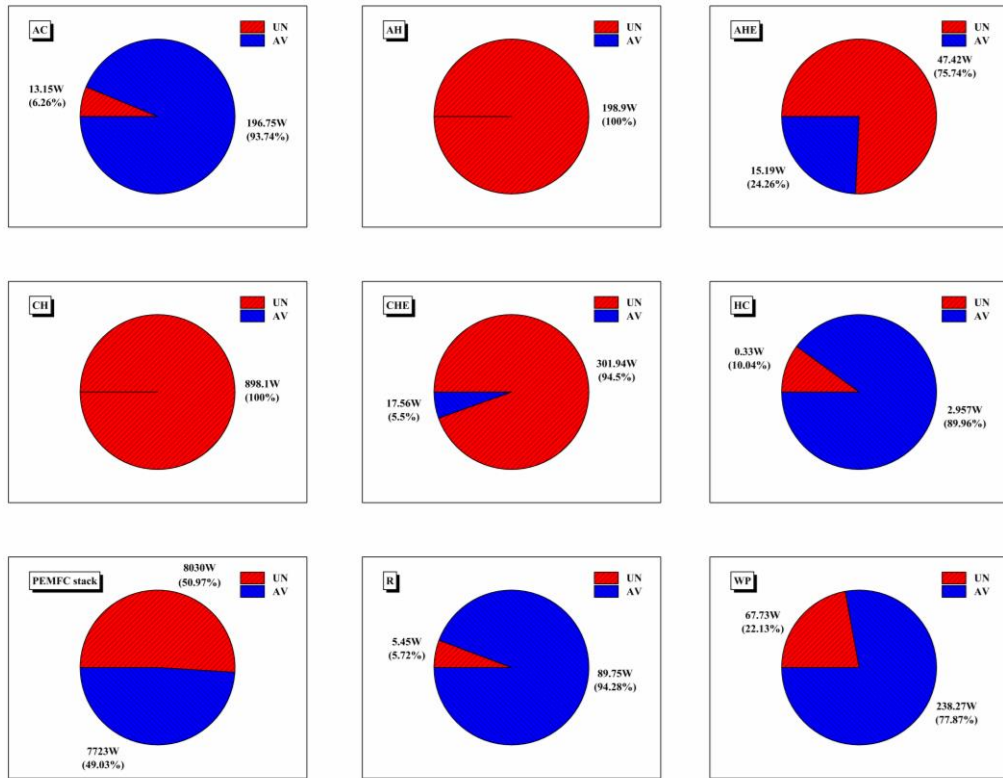


Fig.5. Splitting of unavoidable and avoidable exergy destructions in each single component

PEMFC stack occupies the dominate part (93.25%) in contribution to the avoidable exergy destructions. Order of the auxiliary components in contribution to the avoidable exergy destruction is: WP>AC>R>CHE>AHE>HC. Priority should be given to these components with larger avoidable exergy destruction. Compared with the suggestions from the conventional exergy analysis, a different priority order for improvement is found here. This difference could be explained by the ratios of

unavoidable and avoidable parts as shown in Fig. 5: although exergy destructions in CH and CHE are higher than other components, however, most of the exergy destructions in CH (100%) and CHE (94.5%) are unavoidable. On the other hand, most of the exergy destructions in AC (93.74%), WP (77.87%) and R (94.28%) are avoidable.

A coincidence is found that priority order from the advanced exergy analysis is similar to the order of the power consumption, where AC and WP occupy the higher priority for improvement. Despite the similarity, the advanced exergy analysis with a more complex analysis process provides a more reliable suggestion for system optimization.

4.5. Splitting of the exogenous and endogenous parts

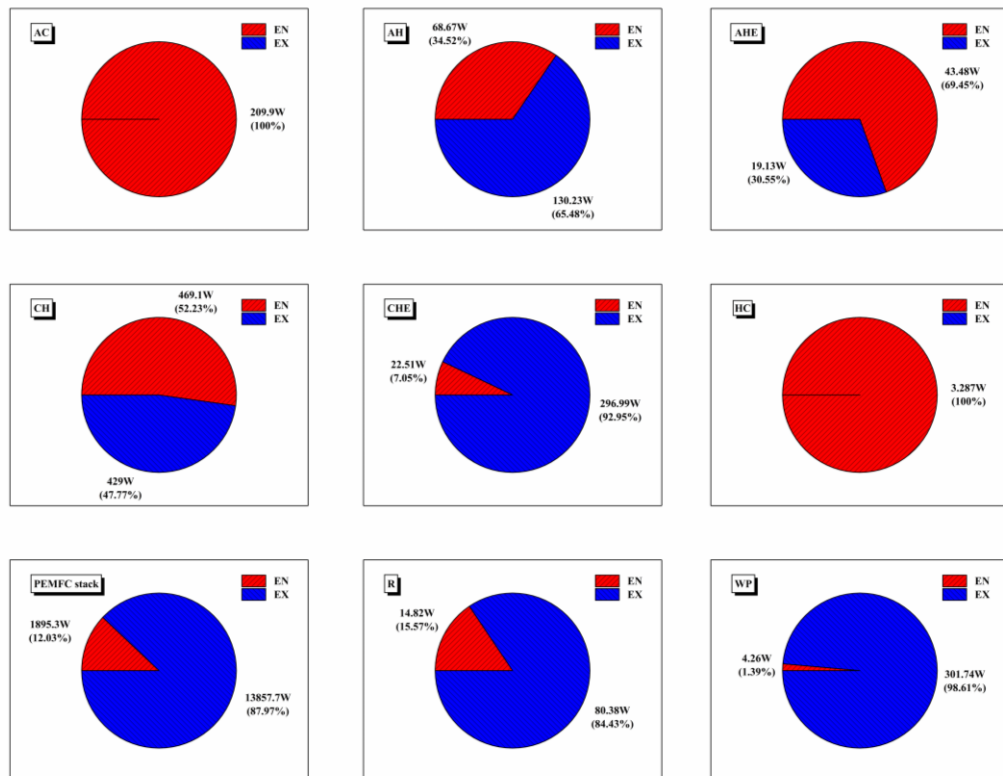


Fig.6. Splitting of exogenous and endogenous exergy destructions in each single component

Conventional exergy analysis could provide information about the exergy

destruction in the individual component; however, it is not able to show the interactions between different components. Advanced exergy analysis could make up this deficiency of conventional exergy analysis. In the PEMFC power system, performance of the core component, i.e. PEMFC stack, is closely connected to other components. Performance of the stack is significantly affected by the operation conditions that are provided by the auxiliary components. Using the engineering method mentioned above, exergy destruction of each component is split into endogenous and exogenous parts as shown in Table 7. Ratios of endogenous and exogenous parts in different components are shown in Fig. 6.

A bigger exogenous exergy value means that the component has stronger interaction with other components. It can be seen that the exogenous part is larger than the endogenous part in PEMFC stack, AH, CHE, R and WP. Exergy destruction of these components would decrease if exergy efficiencies of other components are improved; the endogenous part is larger than the exogenous part in CH, AHE, AC, HC, which means that exergy destructions in these components mainly result from the internal irreversibility of the components themselves. It should be noted that the exogenous exergy destruction of the PEMFC stack occupies large part (77.65%) of the total exergy destruction, which shows that improvement of the auxiliary components would be an efficient approach for the system performance improvement.

4.6. The second level splitting

Results of the second level splitting in the advanced exergy analysis are shown in Table 7. PEMFC stack is still the paramount component in the system, order of the four kinds of exergy destructions in the PEMFC stack is: $E_{d,k}^{UN,EX} > E_{d,k}^{AV,EX} > E_{d,k}^{AV,EN} > E_{d,k}^{UN,EN}$. Since the exogenous avoidable part (6254.82W) is much larger than the endogenous avoidable part (1468.18W), improvement priority should be given to the auxiliary components to order to increase the exergy efficiency of the PEMFC stack.

In the humidifiers, the $E_{d,k}^{UN,EX}$ part are larger than the $E_{d,k}^{EX}$ part, which results in

a negative value of the $E_{d,k}^{AV,EX}$. In the literatures, this unusual phenomenon is explained by: exergy destruction of the humidifiers would increase if performance of other components is improved [26]. Thus, improvement of this kind of components should focus on the components itself. Since $E_{d,k}^{AV,EX}$ in any other components is positive, improvement of the humidifiers would be beneficial to the system optimization as well. However, as elaborated before, all the exergy destruction in the humidifiers are unavoidable due to its inherent reasons. Thus, importance of novel humidification methods should be raised here again.

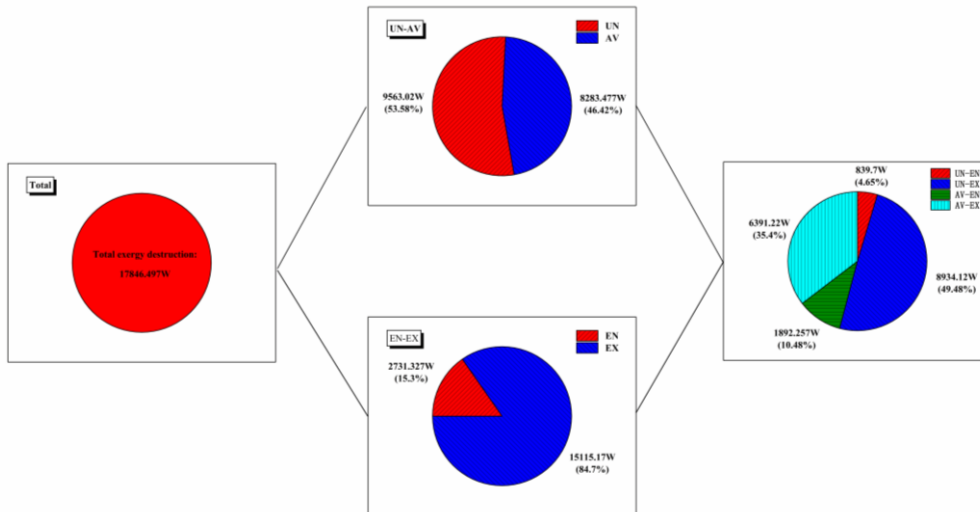


Fig.7. Splitting of total exergy destruction of the PEMFC system

Both AC and WP occupy the relatively large parts of the avoidable part in contribution to the avoidable exergy destructions of the system. However, difference could be found from the second level splitting: all the avoidable exergy destruction in AC is endogenous, while almost all (98.61%) the avoidable exergy destruction in WP is exogenous. Order of these components with less avoidable exergy destruction in contribution to the overall endogenous avoidable exergy destruction is: R>AHE>HC>CHE.

Splitting of total exergy destruction in system level is shown in Fig.7. 46.42% of the total exergy destruction of the PEMFC system (17846.497 W) is avoidable, which

indicates a high improvement potential of the system; 84% of the exergy destruction of the system is exogenous, which indicates a strong intersection between different components in this system. The exogenous avoidable part (35.4%) is higher than that of the endogenous avoidable (10.48%), which show that improvement of the synergy between different components will be a more efficient strategy, rather than focusing on the individual components.

5. Conclusion

A thermodynamic model of a PEMFC power system with parallel-arranged heat recovery strategy is established, and the model is validated rigorously. Based on this model, parameter study of the parallel-arranged heat recovery strategy is presented. Conventional and advanced exergy analyses are conducted on the system. Main findings could be concluded as:

(1) For the parallel-arranged heat recovery strategy, an acceptable interval (0.24-0.56) of stream separation ratio for anode and cathode heat exchangers is found.

(2) Results of conventional exergy analysis show that PEMFC stack are the dominate component with biggest power, biggest fuel exergy, biggest product and biggest exergy destruction. Order of the auxiliary components in contribution to the total exergy destruction is: CH>CHE>WP>AC>AH>R>AHE>HC.

(3) By splitting the exergy destructions into avoidable and unavoidable parts, PEMFC stack still occupies the dominate part in contribution to the avoidable exergy destruction. However, a different order of improvement priority is found among the auxiliary components: WP>AC>R>CHE>AHE>HC.

(4) By splitting the exergy destruction into exogenous and endogenous parts, it is found that exogenous exergy destruction of the PEMFC stack occupies a part of 77.65% from the total exergy destruction, which indicates that improvement of the auxiliary components would be an efficient approach for the system performance improvement.

(5) Values of the exogenous avoidable exergy destruction in both anode and cathode humidifiers are found to be negative, which indicates that improvement priority of this kind of component should be given to the component itself. Due to the

inherent deficiencies of the direct injection method adopted in this system, there is no avoidable exergy destruction in the humidifiers. Thus, development of these novel humidification methods, e.g. membrane humidification method, should be encouraged for the system efficiency improvement.

(6) AC and WP occupy the larger parts of avoidable exergy destruction than other auxiliary components. All avoidable exergy destruction in AC is endogenous, while almost all (98.61%) the avoidable exergy destruction in WP is exogenous.

(7) From the system level, 46.42% of the total exergy destruction is avoidable, which indicates a high improvement potential exists in this system. 84% of the total exergy destruction is exogenous, which indicates a strong intersection between different components in this system.

Notes

The authors declare that there is no conflict of interest.

Acknowledgments

The authors would like to thank the financial support from the China NSF project (NO. 51676209), and Collaborative Innovation Center of Building Energy Conservation and Environmental Control.

References

- [1] Debe MK. Electrocatalyst approaches and challenges for automotive fuel cells. *Nature* 2012;486(7401):43.
<https://doi.org/10.1038/nature11115>.
- [2] Stephens IEL, Rossmeisl J, Chorkendorff I. Toward sustainable fuel cells. *Science* 2016;354(6318):1378-1379.
<http://doi.org/10.1126/science.aal3303>.
- [3] Wang Y, Diaz DFR, Chen KS. Materials, technological status, and fundamentals of PEM fuel cells. *Materials Today* 2019.
<https://doi.org/10.1016/j.mattod.2019.06.005>.
- [4] Wang G, Yu Y, Liu H. Progress on design and development of polymer electrolyte membrane fuel cell systems for vehicle applications. *Fuel Processing Technology* 2018;179:203-228.
<https://doi.org/10.1016/j.fuproc.2018.06.013>.
- [5] Jahnke T, Futter G, Latz A. Performance and degradation of proton exchange membrane fuel cells: state of the art in modeling from atomistic to system scale. *Journal of Power Sources* 2016;304:207-233.
<https://doi.org/10.1016/j.jpowsour.2015.11.041>.
- [6] Yang Z, Du Q, Jia Z. A comprehensive proton exchange membrane fuel cell system model integrating various auxiliary subsystems. *Applied Energy* 2019;256:113959.
<https://doi.org/10.1016/j.apenergy.2019.113959>.
- [7] Yan Q, Toghiani H, Causey H. Steady state and dynamic performance of proton exchange membrane fuel cells (PEMFCs) under various operating conditions and load changes. *Journal of Power Sources* 2006;161(1):492-502.
<https://doi.org/10.1016/j.jpowsour.2006.03.077>.
- [8] Mert SO, Dincer I, Ozelik Z. Performance investigation of a transportation PEM fuel cell system. *International Journal of Hydrogen Energy* 2012;37(1):623-633.
<https://doi.org/10.1016/j.ijhydene.2011.09.021>.
- [9] Huy Quoc Nguyen, Bahman Shabani. Proton exchange membrane fuel cells heat recovery opportunities for combined heating/cooling and power applications *Energy Conversion and Management*.
<https://doi.org/10.1016/j.enconman.2019.112328>
- [10] Mohamed WANW, Kamil MHM. Hydrogen preheating through waste heat recovery of an open-cathode PEM fuel cell leading to power output improvement. *Energy Conversion and Management* 2016;124:543–55.

<https://doi.org/10.1016/j.enconman.2016.07.046>

[11] Liu G, Qin Y, Yin Y. Thermodynamic modeling and exergy analysis of proton exchange membrane fuel cell power system. *International Journal of Hydrogen Energy* 2019.

<https://doi.org/10.1016/j.ijhydene.2019.08.203>.

[12] Bejan A, Tsatsaronis G, Moran MJ. *Thermal design and optimization*. John Wiley & Sons 1995.

[13] Hussain MM, Baschuk JJ, Li X. Thermodynamic analysis of a PEM fuel cell power system. *International Journal of Thermal Sciences* 2005;44(9):903-911.

<https://doi.org/10.1016/j.ijthermalsci.2005.02.009>.

[14] Mert SO, Dincer I, Ozcelik Z. Exergoeconomic analysis of a vehicular PEM fuel cell system. *Journal of Power Sources* 2007;165(1):244-252.

<https://doi.org/10.1016/j.jpowsour.2006.12.002>.

[15] Mert SO, Dincer I, Ozcelik Z. Performance investigation of a transportation PEM fuel cell system. *International Journal of Hydrogen Energy* 2012;37(1):623-633.

<https://doi.org/10.1016/j.ijhydene.2011.09.021>.

[16] Ye L, Jiao K, Du Q. Exergy analysis of high-temperature proton exchange membrane fuel cell systems. *International Journal of Green Energy* 2015;12(9):917-929.

<https://doi.org/10.1080/15435075.2014.892004>.

[17] Tsatsaronis G. Strengths and limitations of exergy analysis, *Thermodynamic optimization of complex energy systems*. Springer, Dordrecht 1999:93-100.

[18] Kelly S, Tsatsaronis G, Morosuk T. Advanced exergetic analysis: Approaches for splitting the exergy destruction into endogenous and exogenous parts. *Energy* 2009;34(3):384-391.

<https://doi.org/10.1016/j.energy.2008.12.007>.

[19] Morosuk T, Tsatsaronis G. A new approach to the exergy analysis of absorption refrigeration machines. *Energy* 2008;33(6):890-907.

<https://doi.org/10.1016/j.energy.2007.09.012>

[20] Morosuk T, Tsatsaronis G. Comparative evaluation of LNG-based cogeneration systems using advanced exergetic analysis. *Energy* 2011;36(6):3771-3778.

<https://doi.org/10.1016/j.energy.2010.07.035>.

[21] Morosuk T, Tsatsaronis G, Boyano A. Advanced exergy-based analyses applied to a system including LNG regasification and electricity generation. *International Journal of Energy and Environmental Engineering* 2012;3(1):1.

<https://doi.org/10.1186/2251-6832-2-1>.

- [22] Tsatsaronis G, Morosuk T. Understanding the formation of costs and environmental impacts using exergy-based methods *Energy security and development*. Springer, New Delhi 2015:271-291.
- [23] Tesch S, Morosuk T, Tsatsaronis G. Advanced exergy analysis applied to the process of regasification of LNG (liquefied natural gas) integrated into an air separation process. *Energy* 2016;117:550-561.
<https://doi.org/10.1016/j.energy.2016.04.031>.
- [24] Morosuk T, Tsatsaronis G. Advanced exergetic evaluation of refrigeration machines using different working fluids. *Energy* 2009;34(12):2248-2258.
<https://doi.org/10.1016/j.energy.2009.01.006>.
- [25] Tsatsaronis G, Morosuk T. Advanced exergetic analysis of a novel system for generating electricity and vaporizing liquefied natural gas. *Energy* 2010;35(2):820-829.
<https://doi.org/10.1016/j.energy.2009.08.019>.
- [26] Morosuk T, Tsatsaronis G. Advanced exergy-based methods used to understand and improve energy-conversion systems. *Energy* 2019;169:238-246.
<https://doi.org/10.1016/j.energy.2018.11.123>.
- [27] Yuan B, Zhang Y, Du W. Assessment of energy saving potential of an industrial ethylene cracking furnace using advanced exergy analysis. *Applied Energy* 2019;254:113583.
<https://doi.org/10.1016/j.apenergy.2019.113583>.
- [28] Wang Z, Xiong W, Ting DSK. Conventional and advanced exergy analyses of an underwater compressed air energy storage system. *Applied Energy* 2016;180:810-822.
<https://doi.org/10.1016/j.apenergy.2016.08.014>.
- [29] Yang Q, Qian Y, Kraslawski A. Advanced exergy analysis of an oil shale retorting process. *Applied Energy* 2016;165:405-415.
<https://doi.org/10.1016/j.apenergy.2015.12.104>.
- [30] Chen J, Havtun H, Palm B. Conventional and advanced exergy analysis of an ejector refrigeration system. *Applied energy* 2015;144:139-151.
<https://doi.org/10.1016/j.apenergy.2015.01.139>.
- [31] Vatani A, Mehrpooya M, Palizdar A. Advanced exergetic analysis of five natural gas liquefaction processes. *Energy Conversion and Management* 2014;78:720-737.
<https://doi.org/10.1016/j.enconman.2013.11.050>.
- [32] Fallah M, Mahmoudi SMS, Yari M. Advanced exergy analysis of the Kalina cycle applied for low temperature enhanced geothermal system. *Energy Conversion and Management*

2016;108:190-201.

<https://doi.org/10.1016/j.enconman.2015.11.017>.

[33] Shaygan M, Ehyaei MA, Ahmadi A. Energy, exergy, advanced exergy and economic analyses of hybrid polymer electrolyte membrane (PEM) fuel cell and photovoltaic cells to produce hydrogen and electricity. *Journal of Cleaner Production* 2019;234:1082-1093.

<https://doi.org/10.1016/j.jclepro.2019.06.298>.

[34] Fallah M, Mahmoudi SMS, Yari M. Advanced exergy analysis for an anode gas recirculation solid oxide fuel cell. *Energy* 2017;141:1097-1112.

<https://doi.org/10.1016/j.energy.2017.10.003>.

[35] Fallah M, Mahmoudi SMS, Yari M. A comparative advanced exergy analysis for a solid oxide fuel cell using the engineering and modified hybrid methods. *Energy Conversion and Management* 2018;168:576-587.

<https://doi.org/10.1016/j.enconman.2018.04.114>.

[36] Chang Y, Qin Y, Yin Y. Humidification strategy for polymer electrolyte membrane fuel cells—A review. *Applied Energy* 2018;230:643-662.

<https://doi.org/10.1016/j.apenergy.2018.08.125>.

[37] Priya K, Sathishkumar K, Rajasekar N. A comprehensive review on parameter estimation techniques for Proton Exchange Membrane fuel cell modelling. *Renewable and Sustainable Energy Reviews* 2018;93:121-144.

<https://doi.org/10.1016/j.rser.2018.05.017>.

[38] Barbir F. PEM fuel cells: theory and practice. Academic Press 2012.

[39] Qian Xu, Lin Liu, Junxiao Feng. A comparative investigation on the effect of different nanofluids on the thermal performance of two-phase closed thermosyphon. *International Journal of Heat and Mass Transfer* 2020;149:119189.

<https://doi.org/10.1016/j.ijheatmasstransfer.2019.119189>.

[40] Qian Xu, Zhenwei Zou, Yushi Chen. Performance of a novel-type of heat flue in a coke oven based on high-temperature and low-oxygen diffusion combustion technology. *Fuel* 2020;267:117160.

<https://doi.org/10.1016/j.fuel.2020.117160>.

[41] Rao Y, Shao Z, Ahangarnejad AH. Shark Smell Optimizer applied to identify the optimal parameters of the proton exchange membrane fuel cell model. *Energy Conversion and Management* 2019;182:1-8.

<https://doi.org/10.1016/j.enconman.2018.12.057>.

[42] Yang S, Xiao Z, Deng C. Techno-economic analysis of coal-to-liquid processes with different

gasifier alternatives. *Journal of Cleaner Production* 2020: 120006.

<https://doi.org/10.1016/j.jclepro.2020.120006>

[43] Liu Z, Xie N, Yang S. Thermodynamic and parametric analysis of a coupled LiBr/H₂O absorption chiller/Kalina cycle for cascade utilization of low-grade waste heat. *Energy Conversion and Management* 2020;205:112370.

<https://doi.org/10.1016/j.enconman.2019.112370>

[44] Tseng CJ, Lo SK. Effects of microstructure characteristics of gas diffusion layer and microporous layer on the performance of PEMFC. *Energy Conversion and Management* 2010;51(4):677-684.

<https://doi.org/10.1016/j.enconman.2009.11.011>.

[45] Fadzillah DM, Rosli MI, Talib MZM. Review on microstructure modelling of a gas diffusion layer for proton exchange membrane fuel cells. *Renewable and Sustainable Energy Reviews* 2017;77:1001-1009.

<https://doi.org/10.1016/j.rser.2016.11.235>.

[46] Wu HW. A review of recent development: Transport and performance modeling of PEM fuel cells. *Applied Energy* 2016;165:81-106.

<https://doi.org/10.1016/j.apenergy.2015.12.075>.

[47] Jiang Y, Yang Z, Jiao K. Sensitivity analysis of uncertain parameters based on an improved proton exchange membrane fuel cell analytical model. *Energy Conversion and Management* 2018;164:639-654.

<https://doi.org/10.1016/j.enconman.2018.03.002>.

[48] Sohani A, Naderi S, Torabi F. Comprehensive comparative evaluation of different possible optimization scenarios for a polymer electrolyte membrane fuel cell. *Energy Conversion and Management* 2019;191:247-260.

<https://doi.org/10.1016/j.enconman.2019.04.005>.

[49] Vuppala RKSS, Chaedir BA, Jiang L. Optimization of Membrane Electrode Assembly of PEM Fuel Cell by Response Surface Method. *Molecules* 2019;24(17):3097.

<https://doi.org/10.3390/molecules24173097>.

[50] Corbo P, Migliardini F, Veneri O. Experimental analysis and management issues of a hydrogen fuel cell system for stationary and mobile application. *Energy Conversion and Management* 2007;48(8): 2365-2374.

<https://doi.org/10.1016/j.enconman.2007.03.009>.

[51] Solsona M, Kunsch C, Ocampo-Martinez C. Control-oriented model of a membrane humidifier for fuel cell applications. *Energy Conversion and Management* 2017;137: 121-129.

<https://doi.org/10.1016/j.enconman.2017.01.036>.

[52] Rodosik S, Poirot Crouvezier J P, Bultel Y. Impact of humidification by cathode exhaust gases recirculation on a PEMFC system for automotive applications. *International Journal of Hydrogen Energy* 2019;44(25): 12802-12817.
<https://doi.org/10.1016/j.ijhydene.2018.11.139>.

[53] Kim B J, Kim M S. Studies on the cathode humidification by exhaust gas recirculation for PEM fuel cell. *International Journal of Hydrogen Energy* 2012;37(5): 4290-4299.
<https://doi.org/10.1016/j.ijhydene.2011.11.103>.